Temporal and Spatial Characterization of Polymer Membrane Deformable Mirrors

Justin D. Mansell* and Brian G. Henderson
Active Optical Systems, LLC, 2021 Girard Ste 150, Albuquerque, NM 87106

ABSTRACT

Effective application of membrane deformable mirrors requires understanding of the operating characteristics of these devices. Using custom developed hardware and software tools, we were able to quantify the temporal and spatial response characteristics of a membrane deformable mirror. Temporal characteristics were analyzed using a frequency sweep stimulus while measuring the DM response on a feedback photodiode. Spatial characteristics of the DM were analyzed in terms of its ability to reproduce Zernike polynomials of increasing order using a variety of actuator patterns. We present here both the techniques for performing these measurements and the results from simulation and the laboratory.

Keywords: Adaptive Optics, Membrane Deformable Mirror

1. INTRODUCTION

Membrane deformable mirrors have been successfully applied to many wavefront control applications including laser beam shaping, atmospheric aberration compensation, and laser machining.[1,2,3] Knowledge of the static and dynamic operating characteristics of these devices is required to determine the suitability of a membrane deformable mirror for a particular application. The temporal response of a membrane DM was characterized by applying a focus shape to a DM with a sinusoidal time varying magnitude. The spatial response was characterized by analyzing a membrane DM's ability to reproduce certain Zernike polynomials. The techniques used to obtain these results are described as well.

2. BACKGROUND

2.1. Membrane Resonance Theory

The theory governing the resonance frequencies of an ideal circular membrane under tension finds that the resonant frequencies are given by[4,5],

$$f_n = C_n \frac{1}{D}\sqrt{\frac{T}{\rho}}$$

where f_n is the resonant frequency, C_n is a constant related to the Bessel functions, D is the membrane diameter, T is the membrane tension, and ρ is the membrane material area density. For the first mode, C_n is 0.76. It is interesting to note that the thickness does not affect the resonance frequency.[5]

Due to the commercial off-the-shelf (COTS) nature of our membranes, we do not know the tension in the membranes during manufacture, but we can use the above equation to solve it for a given measured resonance frequency. We typically see first resonances in a membrane deformable mirror around 500 Hz, so for a polymer material density of ~500 kg/m^3, a thickness of 5 microns, and a diameter of 25 mm, we can estimate the membrane tension to be 0.67 N/m and the membrane stress to be 0.11 MPa.

2.2. Zernike Numbering

In this document we are using the ordering put forth in Malacara's Optical Shop Testing[6] in which the Zernike terms are sorted first by their order (n) and then by their l term. Table 1 shows Zernike order through the third-order terms. In this study we neglected piston.

* Justin.Mansell@mza.com; phone 1 505 245-9970 x122

Order	n	l	Name
1	1	-1	X-Tilt
2	1	1	Y-Tilt
3	2	-2	90° Astigmatism
4	2	0	Focus
5	2	2	45° Astigmatism
6	3	-3	Y Trefoil
7	3	-1	Y Coma
8	3	1	X Coma
9	3	3	X Trefoil

Table 1– Order of the Zernike Terms

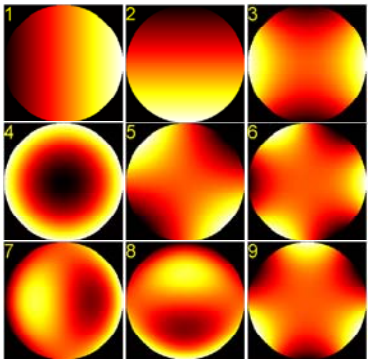

Figure 1 – Zernike terms 1 - 9

3. APPROACH

3.1. Temporal Characterization

Figure 2 shows the experimental setup we used to measure the frequency response of the membrane deformable mirrors. Light from a HeNe laser was expanded with lenses L1 and L2 to fill the DM surface and then sampled with a beam splitter (BS) and lens L3 to illuminate a photodiode (PD). All the actuators were driven with the same voltage in the setup so the mirror surface took on a parabolic (focus) shape.

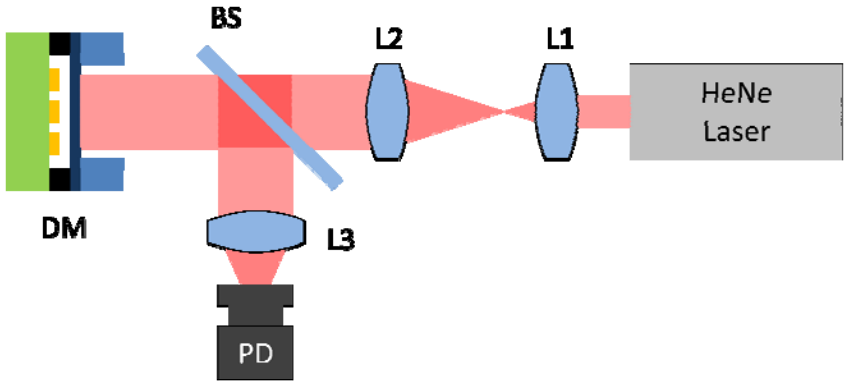

Figure 2 – Optical Setup for Frequency Response Testing

We initially proposed using an interferometer for determining the DM position as a function of applied signal, but the interferometer posed challenges in extracting the signal due to the non-linear response of the photodiode with DM position. Because the membrane DM is a curvature device and the intensity transport equation (ITE) is also a Laplacian, we decided to place an out-of-focus image of the DM onto the photodiode which will give an approximately linear relationship between DM position and photodiode current.

3.2. Spatial Characterization

Two different approaches were taken to analyze the spatial characteristics of a membrane DM. In the first approach, a least squares fit of each of the desired Zernike terms was computed and applied to the DM. In the second approach, a numerical optimization algorithm was used to search the DM actuator space in order to reproduce the desired Zernike term.

Figure 3 shows the actuator patterns we used in this testing. We first generated influence functions for four different deformable mirrors on a 128x128 pixel grid with about a 0.21-mm spacing such that the DM aperture was represented with a small guard-band. Our 1" membrane deformable mirrors have about 10

microns of focus throw on average, so we normalized the influence functions such that the sum of all of the commands produced 10 microns of focus throw over the aperture. We then limited our simulation to only use the inner 80% of the mirror since the edges are typically poorly controlled.

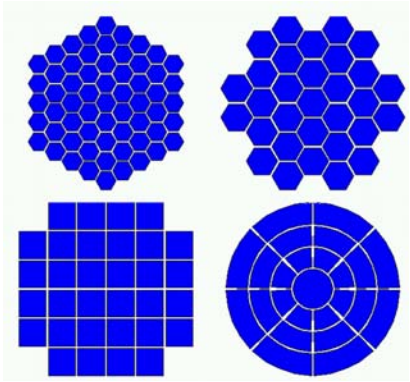

Figure 3 – Four patterns of deformable mirror actuators used in Zernike fit testing

3.2.1. Matrix Fitting of Zernike Terms

In this approach, a least squares matrix fit of the desired DM shape using the DM influence functions was computed for each Zernike term. The procedure is as follows:

1. Create a "poke" matrix *P* using the simulated influence functions of the membrane DM
2. Compute the pseudo-inverse of *P* using the Singular Value Decomposition (SVD) to create a phase-space control matrix *C*
3. Compute the phase profile for the desired Zernike term
4. Multiply the control matrix *C* by the desired phase profile to obtain weights (forces) for each of the influence functions.

We then scaled the forces such that they were between 0 and 1 by subtracting the minimum and then dividing by the maximum. We did not allow any negative forces because the electrostatic actuators on the membrane DMs can only pull on the membrane and cannot push (the effective pushing force is obtained from the tension in the membrane). We then created the phase profile by adding together each of the weighted influence functions. To better see the desired aberration, we also removed the focus term that is the bias condition of the membrane deformable mirror.

3.2.2. Metric Searching to Maximize Zernike Overlap Integral

After doing the matrix-based fitting, we implemented a genetic search algorithm to maximize the overlap integral between a deformable mirror shape and a given Zernike term. We implemented the Guided Evolutionary Simulated Annealing (GESA) algorithm in which a set of families of solutions are tried and the best solution becomes the parent for the next generation. Each child of the parent is generated as a random perturbation of the parent with a uniform random number generator with a radius equal to the maximum throw of the device initially. The random radius was reduced by a simulated annealing factor each iteration.

4. RESULTS

4.1. Temporal Frequency Response

We made measurements of several different membranes by exciting the DM with a sinusoidal signal and measuring the response on the photodiode. Figure 4 shows the frequency response of two 1" diameter membranes with different tensions. From this data we concluded that there are at least two phenomena

acting together to produce this transfer function. On this plot we chose to use the electrical engineering convention of $20*\log_{10}(V)$ for the vertical axis. Before the first resonance of the mirror membrane, which is around 1 kHz, we see an approximate $1/f^{0.25}$ reduction in frequency response. We believe that this is primarily due to air damping. After the resonance(s), the fall-off in frequency response fits well to an f^{-4} curve. Based on this fall-off rate, we believe that we are seeing two resonances in the data before the rapid fall-off.

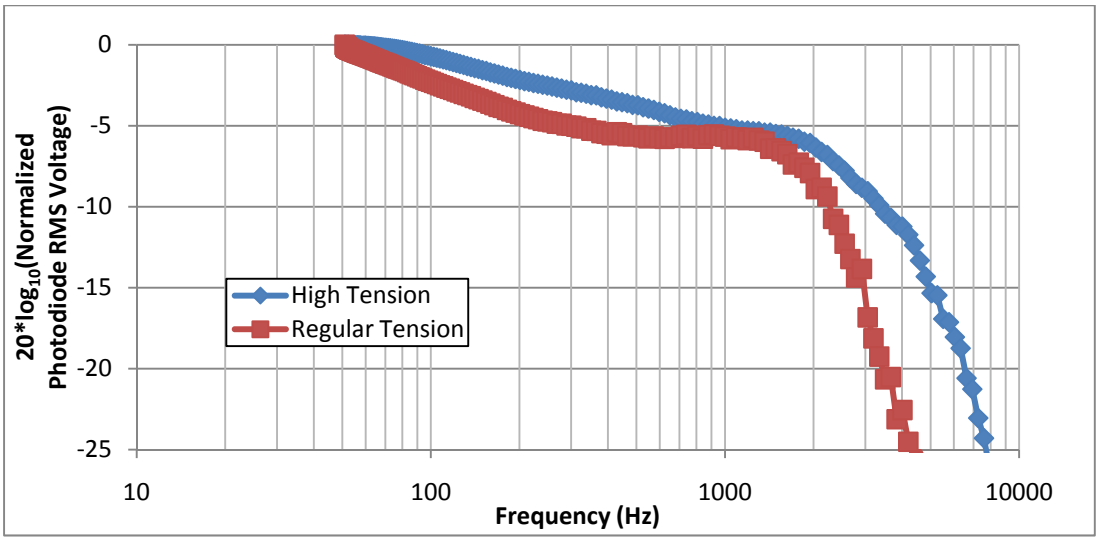

Figure 4 – Measured membrane DM response on a photodiode

In addition to the high-speed testing, we also did some long-term drift testing. In this case, we replaced L3 with a 5x reimaging telescope and replaced the photodiode in the experimental setup shown in Figure 2 with our Shack-Hartmann Wavefront sensor based on an Allied Vision Technologies Marlin F131b camera. The mirror was biased to about half of its throw and the curvature was monitored over one evening and into the morning. A frame was taken from the wavefront sensor every 30 seconds during the test. Figure 5(a) shows the fit to the focal power measured by the wavefront sensor in the x and y axes in the DM space (compensating for the 5x telescope). Figure 5(b) shows three coefficients of a Zernike decomposition of the wavefront measured by the wavefront sensor. In both plots we observe an oscillation at a very low frequency which we believe corresponds to the activation of the air conditioning units in the lab. The oscillation does not significantly affect the x and y tilts, but the tilt terms do drift as a function of time. The focal power is the same in magnitude in the x and y axes meaning that the shape drift is not astigmatic (at 90-degrees), but is focus. The magnitude of the focus drift is ~0.01 diopters on the DM, which corresponds to about 100 m of curvature.

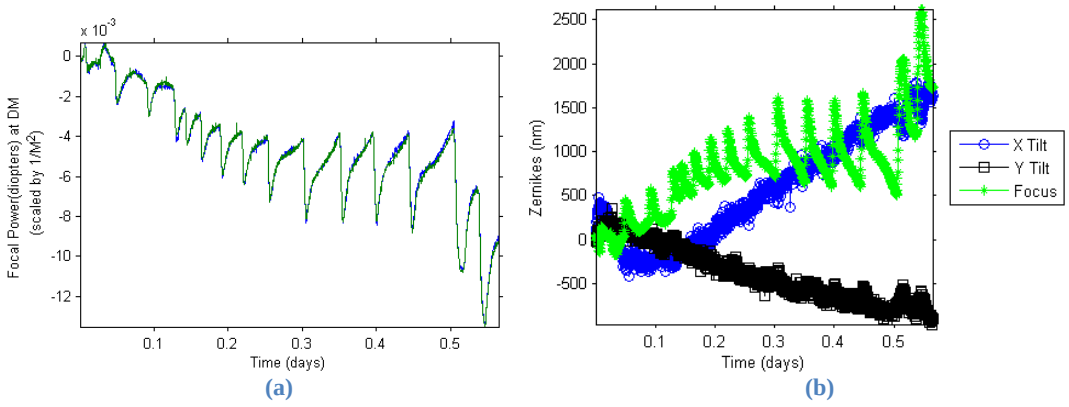

Figure 5 – Results of long-term drift testing of a biased membrane deformable mirror showing the change in (a) the focal power in the two axes and (b) a decomposition of the shape into tilt and focus.

4.1.1. Comments on Environmental Factors

There are three environmental factors that contribute significantly to the performance of a membrane deformable mirror's frequency response: air damping, temperature, and humidity. Each of these will be discussed below.

4.1.1.1. Air Damping

The frequency response measurements showed a slight reduction in the performance of the mirror as a function of frequency well before a resonance occurs. There is evidence for this kind of damping in the literature[7]. In the future we intend to confirm this by running the same tests on the mirror in a reduced pressure environment.

4.1.1.2. Temperature

We are currently trying to establish the effect of temperature alone on the mirror membranes, but suspect that the long-term drift that we see in the membrane bias curvature over time is related to temperature changes.

4.1.1.3. Humidity

Nitrocellulose membranes tend to take on water vapor from the air. This effect tends to reduce the tension in the membrane and thereby reduce its spring constant restoring force and the resonance frequencies.

There are several ways to mitigate the effects of humidity. One is to change the mirror membrane material. There are several literature sources that have used other materials for optical quality membranes. Another is to seal the membrane with a coating like a metal thin film on both surfaces. Finally, both air damping and humidity can be mitigated with a low-pressure vacuum chamber.

4.2. Matrix Fitting to Zernike Polynomials

Presented here is the analysis of the results of the matrix fitting based approach for reproducing Zernike polynomials with a membrane deformable mirror. Figure 6 shows one example result in which we used the matrix fitting approach to compute influence function weights to generate 90° astigmatism on the annular actuator DM.

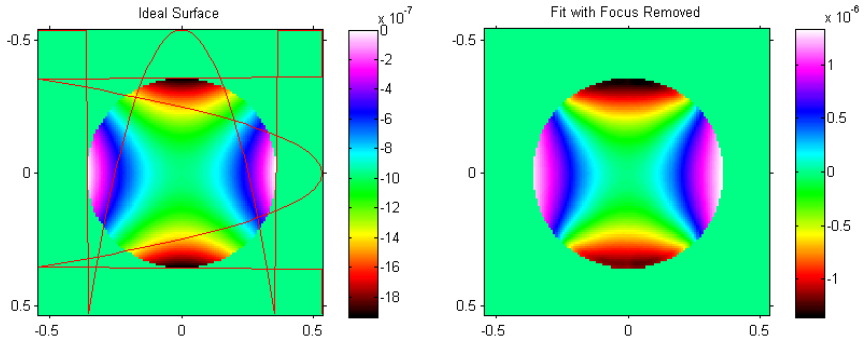

Figure 6 - Result obtained for using the annular actuator deformable mirror to create 90-degree astigmatism

Once we had obtained the phase surface that best created the desired aberration, we did an overlap integral decomposition of the generated phase profile with the each of the 40 Zernike terms. This was done for each mirror for each of the 40 Zernike terms. Figure 7 shows the results obtained from the 25-channel annular actuator deformable mirror. The focus bias was not removed for in these results, so there is a Zernike 4 term in all of the results.

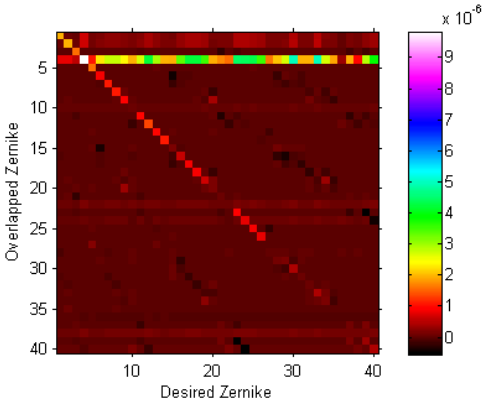

Figure 7 - Results of decomposing the attempt to create Zernike terms using a 25-actuator annular deformable mirror without removing the focal bias.

To determine the ability of each mirror to create each mode, we looked at the diagonal of the matrix (Figure 7) relating desired Zernike term to the overlapped Zernike result. Figure 8 shows the results plotted on a log-scale with the vertical axis limited to 0.1 microns. There were several different trends identified in this experimentation. First, we found that the annular actuator grid was better than all the others at some patterns, but was much worse at others. The annuli were segmented into eight pieces, so the aberrations that matched well to this arrangement of actuators were much better, while those with other angular content (60° angles for example) were much worse. We also were surprised by the 61-actuator device doing more poorly at representing the desired patterns than the lower actuator counts.

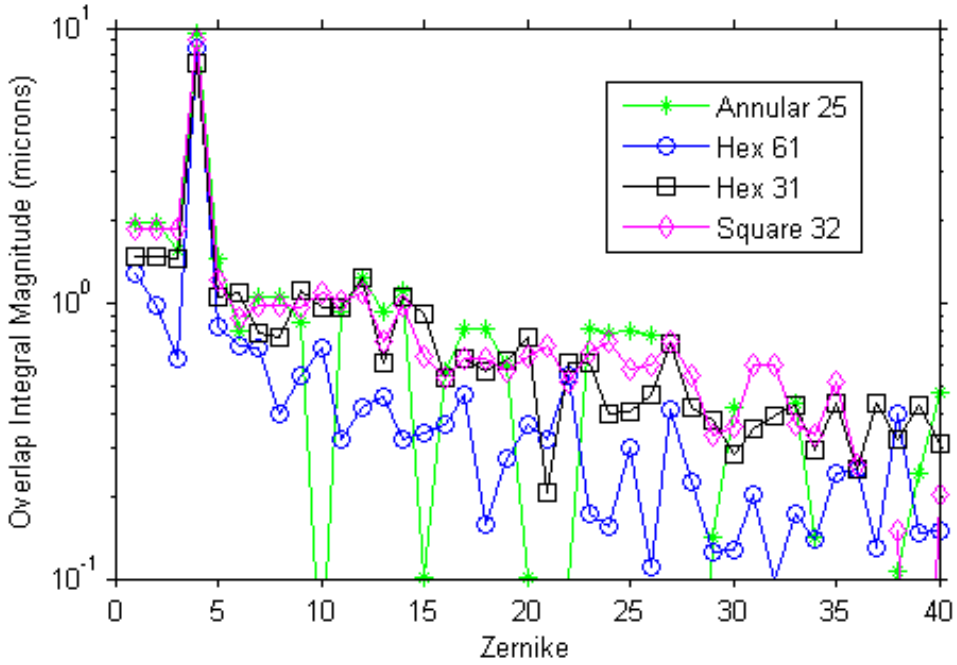

Figure 8 - Magnitude obtained for each of the first 40 Zernike terms with each of the deformable mirrors.

4.3. Metric Search for Reproducing Zernike Polynomials

We used 10 families of solutions with a 98% simulated annealing factor per generation. Each family had as many children as it had actuators. We propagated at least 150 generations, but as many as 3 times the number of actuators. We limited the used area of the deformable mirror to the 80% radius of the device and the throw of the entire device to 10 microns of focus. We also extended our search to include the 59-actuator annular DM and the 61-actuator square grid DM shown in Figure 9. We also extended our search to 60 Zernike terms for the higher actuator count pad array patterns. We only considered positive amplitude Zernike terms in this test.

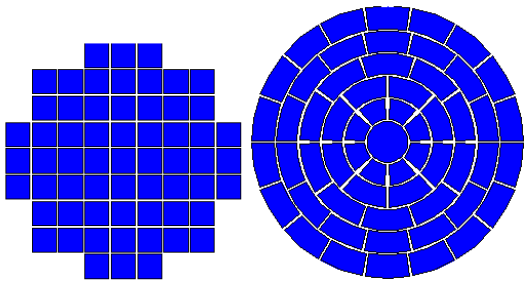

Figure 9 - Higher Actuator Count DM Pad Arrays

We did not try to minimize any of the other Zernike terms during our search, so we did see some coupling to higher-order terms to maximize the desired term. For example, with the 25-actuator annular DM (center actuator and 3 rings of 8 segments), we found the focus-removed x-tilt term with maximum overlap integral to the Zernike term was the shape shown in Figure 10. Figure 11 shows the decomposition of the non-focus-removed tilt term. This decomposition clearly has a large tilt term (the #1 Zernike), but also significant focus due to the nature of the membrane DM and some trefoil and x-coma.

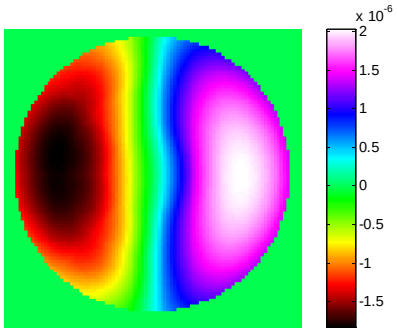

Figure 10 - Best focus-removed x-tilt term from the 25-actuator annular pad array

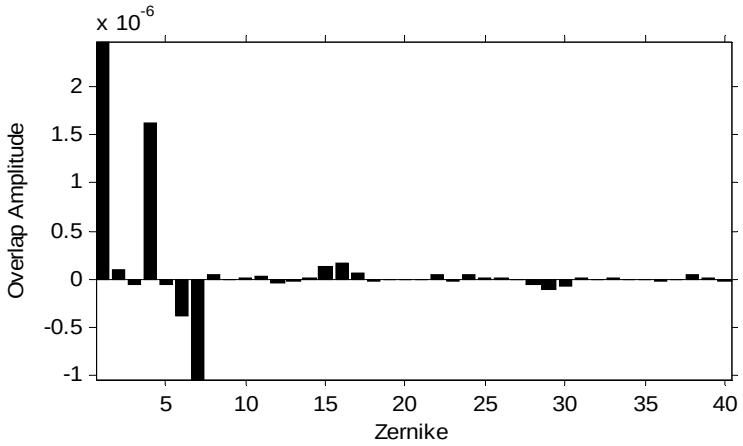

Figure 11 - Zernike decomposition of the best x-tilt term obtained from the 25-actuator annular pad array using the GESA search.

Figure 12 shows the results of the Zernike overlap metric search. The results were very similar in nature to the matrix-based results presented above. The mirror was again clearly better at low spatial frequency terms than it was at higher spatial frequency terms.

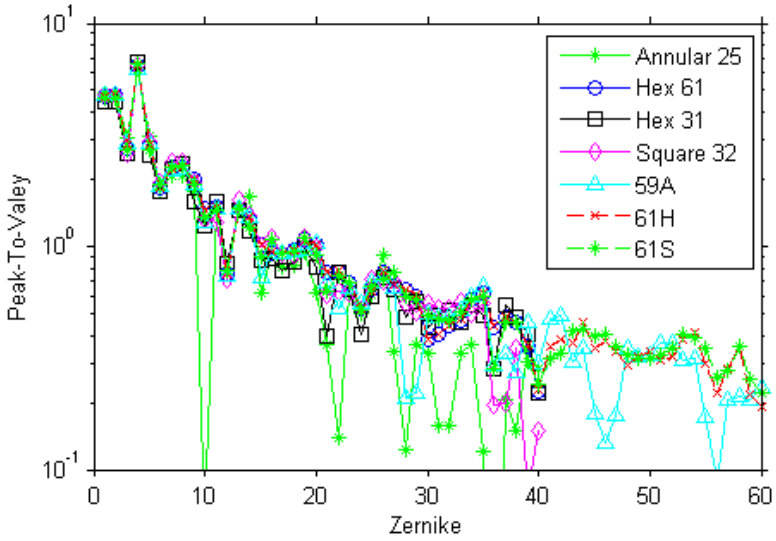

Figure 12 - Peak-to-valley amplitude of each of the Zernike terms tested for each of the pad arrays tested.

The pad array patterns that appeared to do the best at creating all the different Zernike terms were the 61-actuator hex and square grid patterns. The 25 and 59 actuator annular patterns were the worst in our testing due primarily to significant drop-outs on some Zernike terms.

We did some analysis to determine the reason the 25-actuator annular DM did so poorly in representing the Zernike terms in some of the cases. We started with the lowest order term that was doing poorly, which was the 10^{th} Zernike term. Figure 13 shows the shape of the Zernike term and the actuator pattern. The problem clearly stems from the fact that the actuators line up exactly with the nulls in the Zernike term. We found a similar result in Zernike #21, the next poorly performing Zernike.

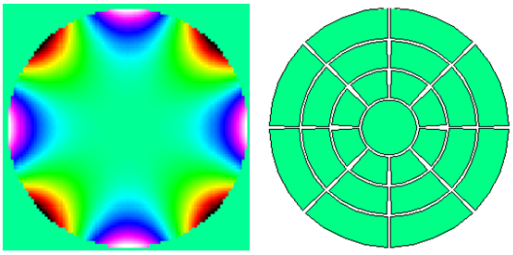

Figure 13 - Zernike 10 and the actuator pattern for the 25-actuator annular DM.

Zernike Amplitude Reduction Analysis

The result in Figure 12 clearly shows that the maximum amplitude of the Zernike term reduces with the Zernike number. The DM is not as able to excite higher order terms as well as it is lower order terms. To analyze this phenomenon we averaged the maximum amplitude of the Zernike terms with like radial powers for all the higher actuator count (>32) DMs. Figure 14 shows the results as both linear and log scale plots. The average amplitude falls-off as a -1.6 power law.

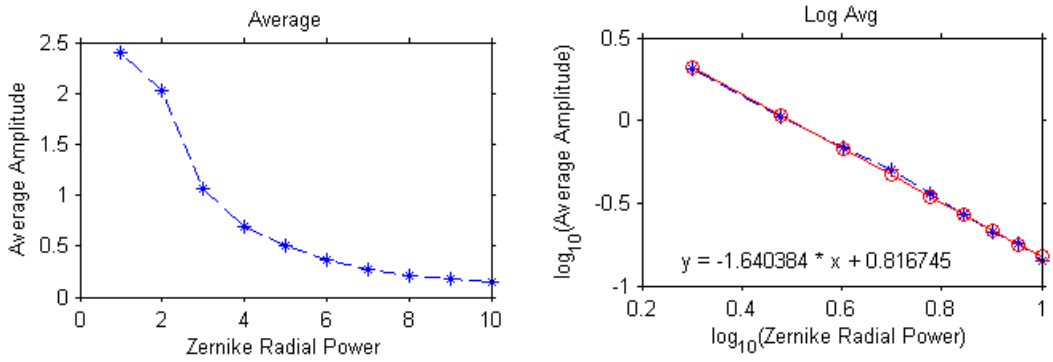

Figure 14 - Analysis of the Average Maximum Amplitude with respect to Zernike Radial Power

5. CONCLUSIONS AND FUTURE WORK

The polymer membrane deformable mirror testing results presented here show that these DMs can operate at a relatively high frequency and produce shapes that are relevant to many applications such as generating Kolmogorov phase screens and laser beam shaping. Several deleterious environmental effects were identified during testing and evaluation including the speed decrease from air damping and tension reduction due to humidity. We plan to investigate different environmental compensation techniques in future work.

REFERENCES

[1] D. Dayton et al., "Characterization Of A Novel Electro-Static Membrane Mirror Using off-the-Shelf Pellicle Membranes", Conference on Adaptive Optics for Industry and Medicine 2007 (Galway, Ireland)

[2] B. G. Henderson et al., "Laser Beam Shaping with Membrane Deformable Mirrors", SPIE Vol. 7093 (2008).

[3] J. Mansell et al., "High Power Deformable Mirrors", SPIE Conference Mirror Technology Days 2007.

[4] T. D. Rossing, F. R. Moore, and P. A. Wheeler, [The Science of Sound, 3rd Edition], Addison Wesley, San Francisco, 283-4 (2002).

[5] Ronald P. Grosso and Martin Yellin, "The membrane mirror as an adaptive optical element," J. Opt. Soc. Am. 67, 399-406 (1977)

[6] Malacara, D., [Optical Shop Testing], Wiley-Interscience, (1992).

[7] T. G. Bifano and J. B. Stewart, "High-speed wavefront control using MEMS micromirrors", Proc. SPIE 5895-27, (2005).